Science Advances
AAAS

advances.sciencemag.org/cgi/content/full/6/23/eaaz0742/DC1

Supplementary Materials for

Proximo-distal positional information encoded by an Fgf-regulated gradient of homeodomain transcription factors in the vertebrate limb

Irene Delgado, Alejandra C. López-Delgado, Alberto Roselló-Díez, Giovanna Giovinazzo, Vanessa Cadenas, Laura Fernández-de-Manuel, Fátima Sánchez-Cabo, Matthew J. Anderson, Mark Lewandoski, Miguel Torres*

*Corresponding author. Email: mtorres@cnic.es

Published 3 June 2020, *Sci. Adv.* **6**, eaaz0742 (2020)
DOI: 10.1126/sciadv.aaz0742

This PDF file includes:

Figs. S1 to S10

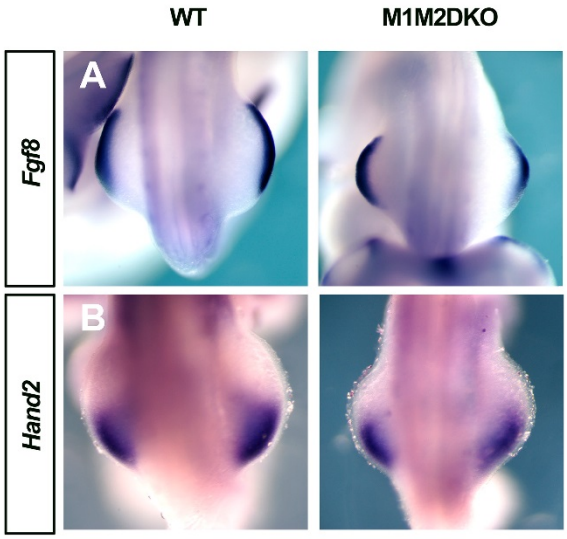

Figure S1. Limb initiation and AP patterning are not affected in *M1M2DKO* embryos. (A) *Fgf8* (N=1/1) and (B) *Hand2* (N=2/2) expression in *WT* and *M1M2DKO* E10.5 HLs showing that limb initiation and AP prepatterning occurs normally in the mutants.

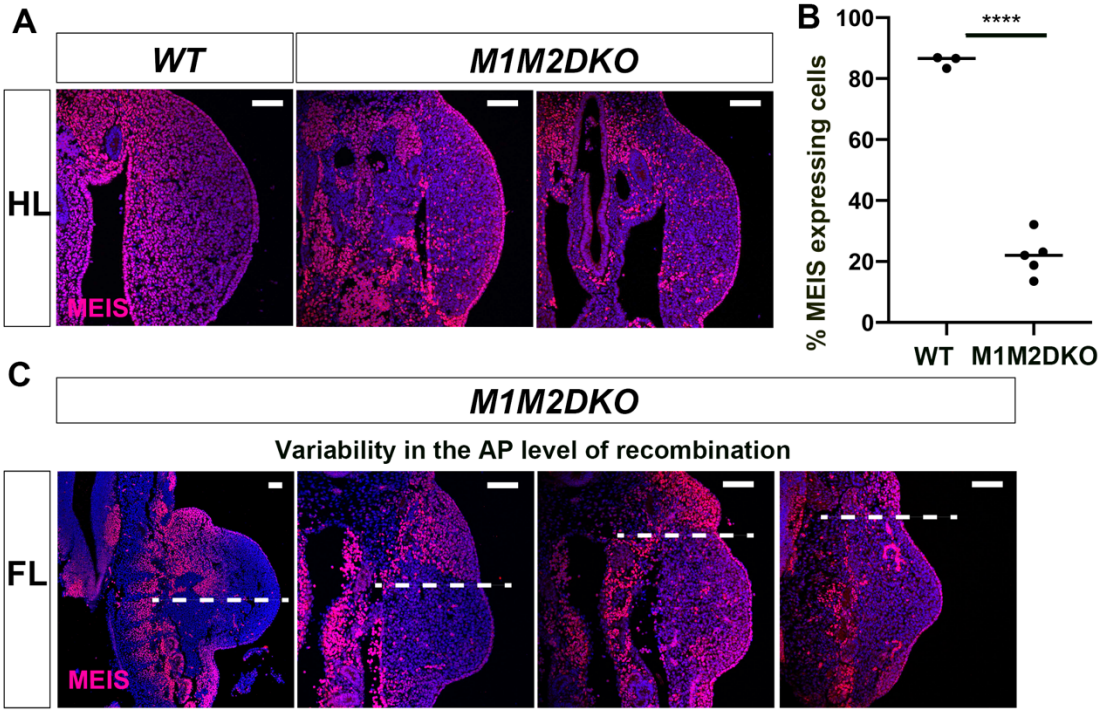

Figure S2. Pattern and percentage of recombination of Dll1Cre and variability in the axis AP level. (A) MEIS immunofluorescence in *WT* and *M1M2DKO* HLs. (B) Quantification of MEIS expressing cells in the *WT* and *M1M2DKO* HLs show around 75% decrease of MEIS expressing cells in the mutant. 3 WT and 5 DKO limbs were quantified. Statistical comparisons were performed using an unpaired t-test. P value < 0,0001 (C) MEIS distribution in *M1M2DKO* FLs showing the different AP levels of recombination between them. White dashed lines label the most anterior border of recombination in the limb. Scale bar = 100µm

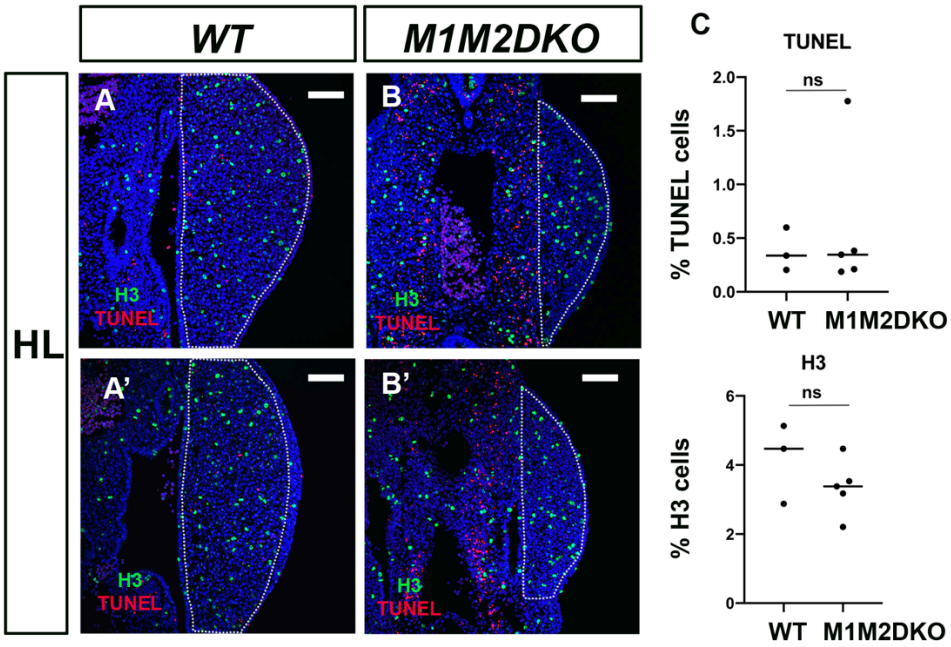

Figure S3. Differences in cell death or proliferation do not account for *M1M2DKO* HL skeletal phenotype. H3 immunostaining and TUNEL staining in WT (A-Aa) and *M1M2DKO* (B-Ba) HLs at E10.5. (C) Quantification of TUNEL and H3 positive cells show that there is no significant proliferation or cell death in *M1M2DKO* HLs. The region of interest used for quantification has been indicated with a dotted white line and includes limb bud mesenchyme distal to the celomic epithelium. Statistical comparisons were performed using an unpaired t-test. Scale bar = 100μm

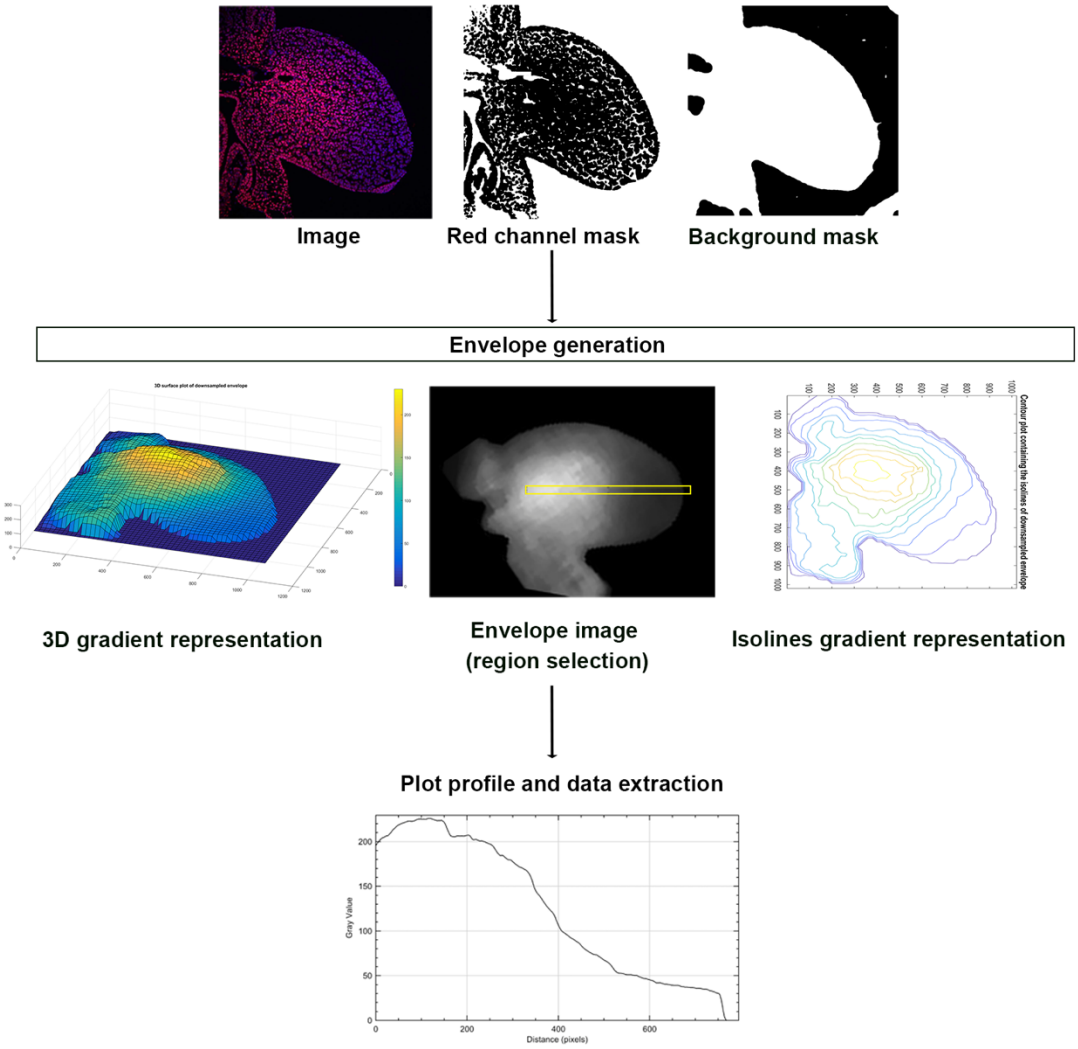

Figure S4. Envelope generation and data extraction workflow. From the image, a mask in the Meis channel was created eliminating the ectoderm and blood cells. Another mask was created for the background. The envelope image was generated with MATLAB by sampling the intensity of pixels included within the intersection of the foreground and the mask in the Meis channel (described in more detail in Materials and Methods). 3D gradient representation shows high intensity Meis levels in yellow. The isolines image represent points with the same intensity. From the envelope image, a rectangular region 30pixels broad from proximal to distal is selected in ImageJ and the intensity plot profile generated. Data are extracted from this plot in which Y axis is relative intensity of Meis and X axis represent the PD length of the limb.

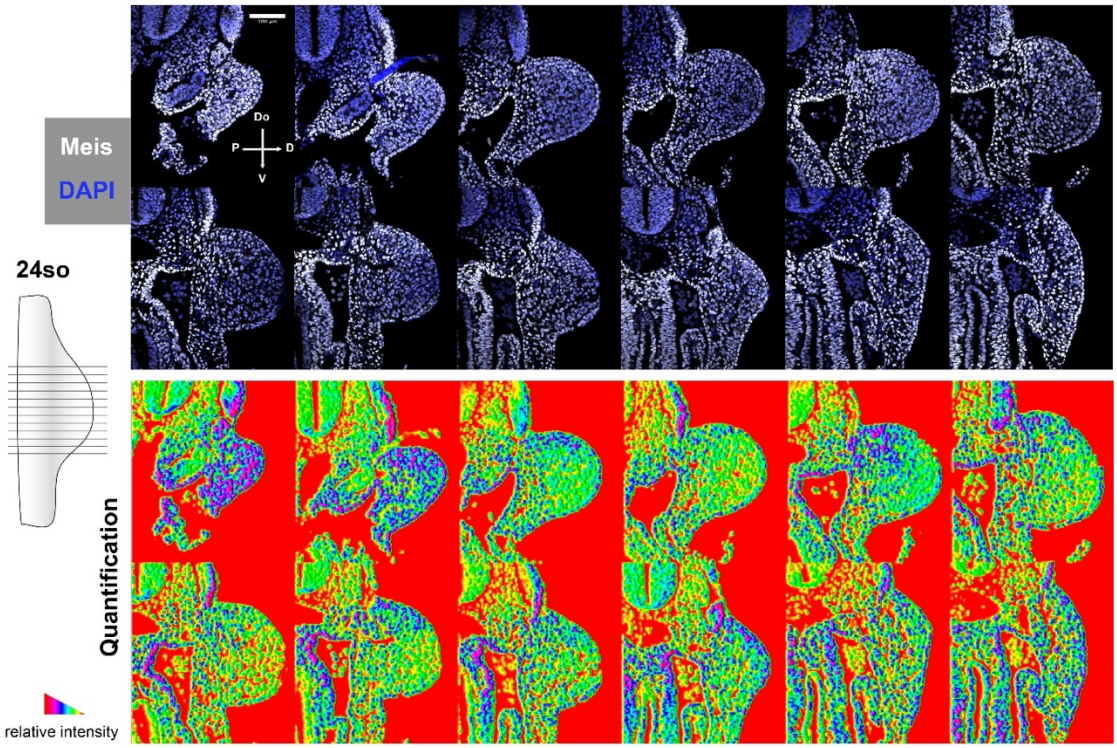

Figure S5. Serial longitudinal sections along the AP dimension of a 24so limb bud. On the left, a schematic representation of the sectioning strategy. Upper images show Meis immunofluorescence (white) and DAPI (blue) and lower images show the corresponding color-coded representation of MEIS relative intensities. Scale bar = 100µm. P: proximal, D: distal, Do: dorsal, V: ventral

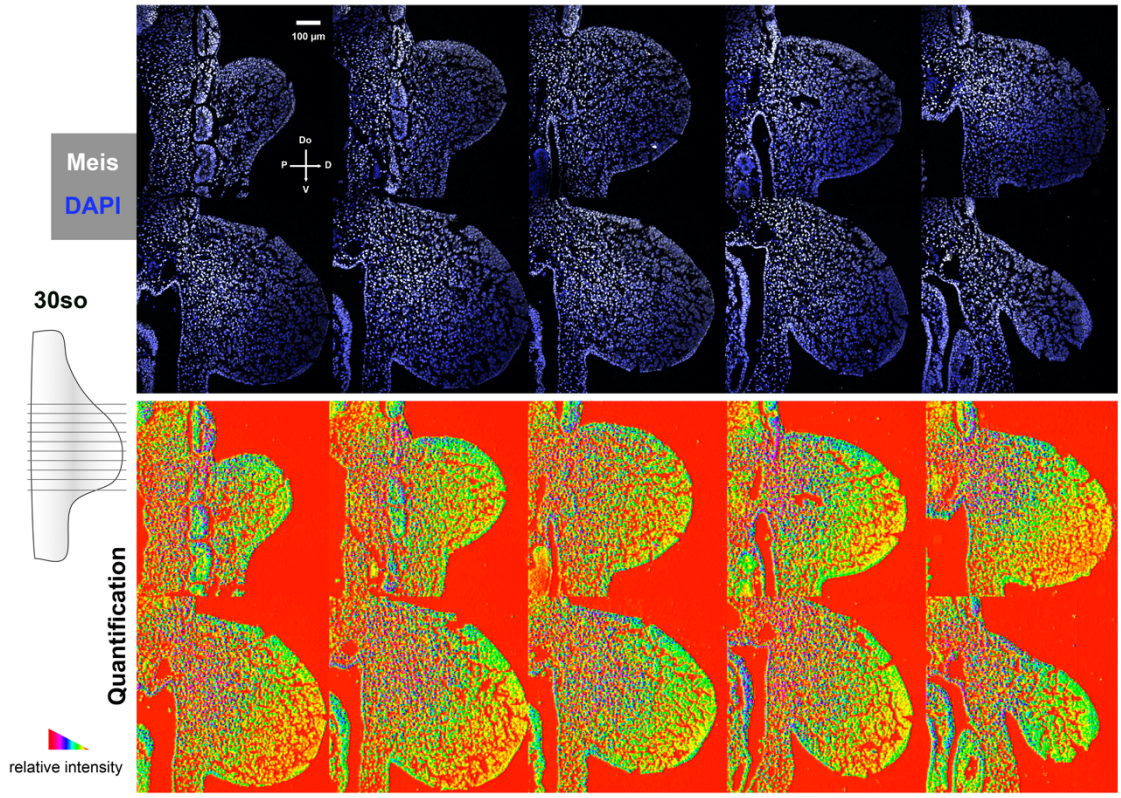

Figure S6. Serial longitudinal sections along the AP dimension of a 30so limb bud. On the left, a schematic representation of the sectioning strategy. Upper images show Meis immunofluorescence (white) and DAPI (blue) and lower images show the corresponding color-coded representation of MEIS relative intensities. Scale bar = 100µm. P: proximal, D: distal, Do: dorsal, V: ventral

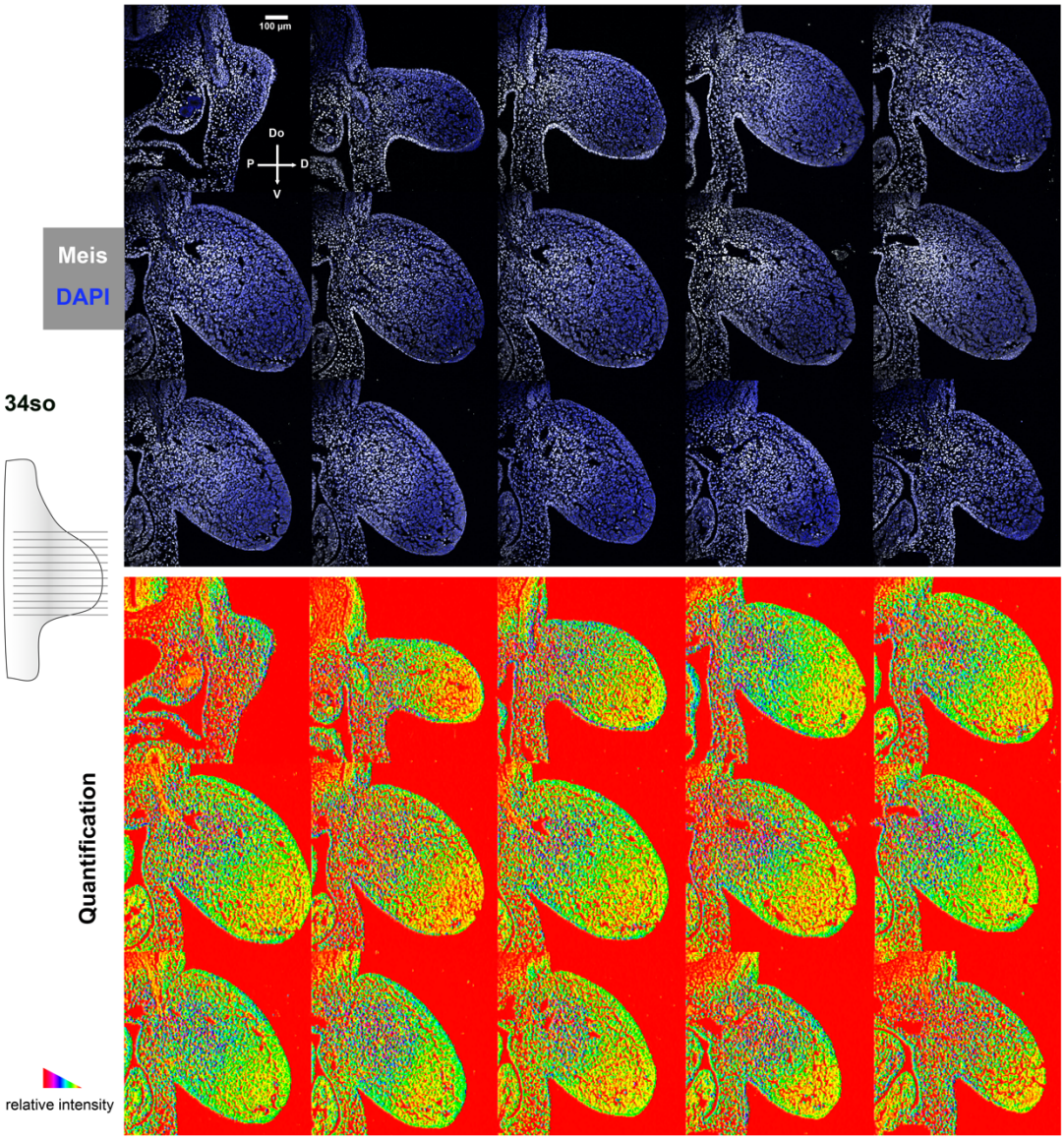

Figure S7. Serial longitudinal sections along the AP dimension of a 34so limb bud. On the left, a schematic representation of the sectioning strategy. Upper images show Meis immunofluorescence (white) and DAPI (blue) and lower images show the corresponding color-coded representation of MEIS relative intensities. Scale bar = 100µm. P: proximal, D: distal, Do: dorsal, V: ventral

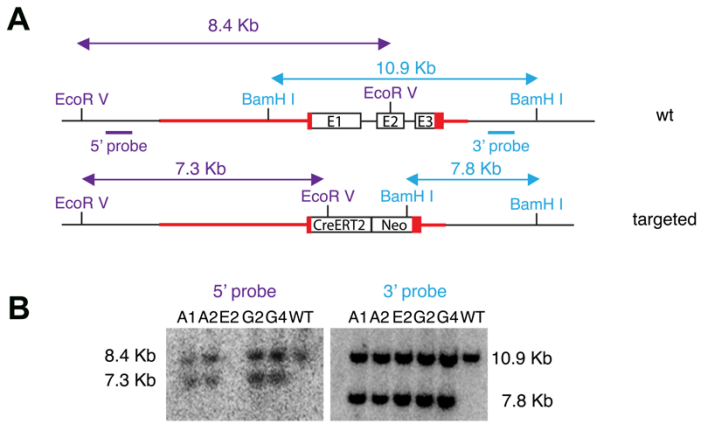

Figure S8. *HoxA13*^{CreERT2} generation. (A) A Cre-ERT2-FRT-Neo-FRT-LoxP cassette was inserted into exon 1 just downstream of the endogenous ATG, replacing 1864 bps of the coding region spanning exons 1 and 2. The short homology arm extends 2.22kb downstream of the 3' end of the FRT-Neo-FRT-LoxP cassette. The long homology arm ends at the 5' side of the Cre-ERT2 gene and is ~6.03kb long. (B) Neomycin-resistant ES-cell clones were screened by Southern blot.

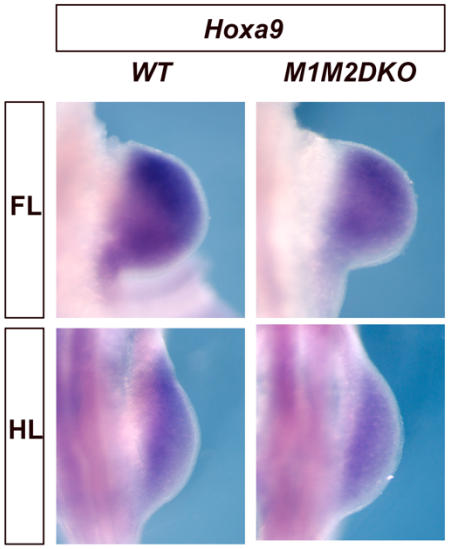

Figure S9. *Hoxa9* is normally expressed in *M1M2DKO* limbs. E10.5 FL and HLs of *WT* and *M1M2DKO* are shown with no difference in *Hoxa9* pattern of expression (n=2/2).

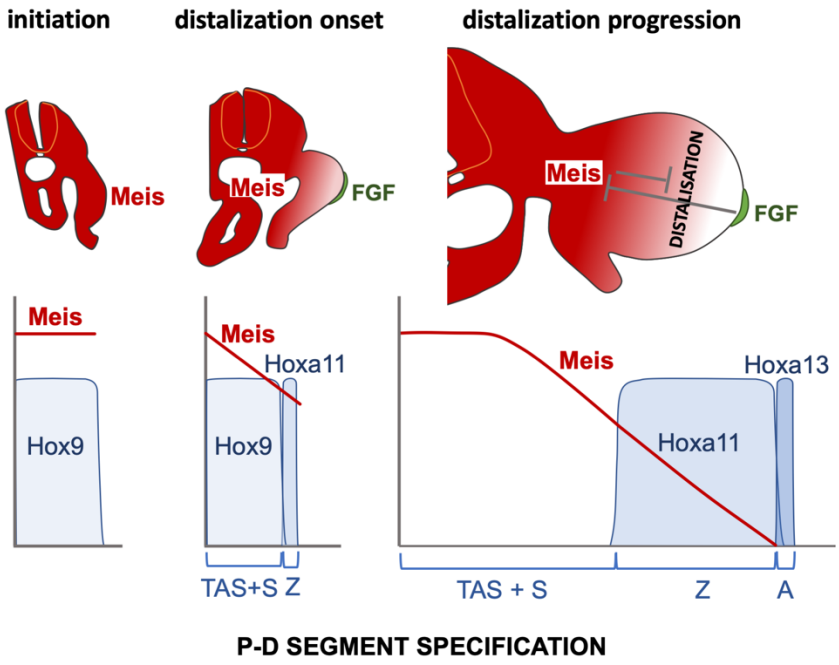

Figure S10. Model for PD segment specification dependent on Meis gradient. During limb initiation, Meis is distributed homogenously through the whole PD extension of the limb bud. At this stage *Hox9-10* paralog genes are responsible for proximal specification. As FGFs initiate their expression in the AER and the limb bud grows, Meis is inhibited by distal signals, which creates a gradient of Meis protein abundance that progressively gets steeper. The evolution of the Meis gradient leads to progressive distalization through HoxA cluster activation. When Meis abundance decreases enough in the distal region to activate *Hoxa11*, zeugopod specification occurs. As limb growth progresses, the gradient evolves until a Meis-negative region is produced at the distal limb bud, which allows *Hoxa13* activation and autopod specification. TAS: trunk appendicular skeleton, S: stylopod, Z: zeugopod, A: autopod.